Article:

Manipulation of fluid flow direction in microfluidic paper-based analytical devices with an ionogel negative passive pump

Tugce Akyazi, Nerea Gil-González, L. Basabe-Desmonts, E. Castaño, M.C. Morant-Miñana, Fernando Benito-Lopez,

Sensors and Actuators B: Chemical 247 : 114–123 (2017)

Manipulation of Fluid Flow Direction in Microfluidic Paper-Based Analytical Devices with an Ionogel Negative Passive Pump

Tugce Akyazi,[1, 2] Nerea Gil-González,[3] L. Basabe-Desmonts,[4, 5] E. Castaño,[3] M.C. Morant-Miñana,[6] Fernando Benito-Lopez[1,7]*

[1] Analytical Microsystems & Materials for Lab-on-a-Chip (AMMa-LOAC) Group, Microfluidics Cluster UPV/EHU, Analytical Chemistry Department, University of the Basque Country UPV/EHU, Vitoria-Gasteiz, Spain.

[2] University of Navarra, TECNUN, Spain.

[3] CEIT and Tecnun (University of Navarra), Donostia-San Sebastián, Spain.

[4] BIOMICs microfluidics, Microfluidics Cluster UPV/EHU, Lascaray Ikergunea Research Center, University of the Basque Country UPV/EHU, Vitoria-Gasteiz, Spain.

[5] Ikerbasque, Basque Foundation for Science, 48011 Bilbao, Spain.

[6]CIC nanoGUNE Consolider, Donostia-San Sebastián, Spain.

[7]Insight Centre for Data Analytics, National Centre for Sensor Research, Dublin City University, Dublin, Ireland.

Abstract

Microfluidic paper-based analytical devices (µPADs) are relatively new group of analytical tools that represent an innovative low-cost platform technology for fluid handling and analysis, enabling simple fabrication/operation and equipment independence and provide a wide range of applications.

Nonetheless, µPADs lack in the effective handling and controlling of fluids, which leads to a main drawback for their reproducibility in large volumes during manufacturing, their transition from laboratory into the market and thus accessibility by the end-users. Herein we investigate the applicability of ionogel materials based on a poly(*N*-isopropylacrylamide) gel with the 1-ethyl-3-methylimidazolium ethyl sulfate ionic liquid as fluid flow manipulator in µPADs using the ionogel as a negative passive pump to control the flow direction in the device. A big challenge undertook by this contribution is the integration of the ionogel materials into the µPADs. Finally,

the characterisation and the performance of the ionogel as a negative passive pump were demonstrated**.**

Keywords: ionogel; passive pump; microfluidic paper-based analytical device; poly(*N*-isopropylacrylamide, ionic liquid.

1. Introduction

Ionic liquids (ILs) are drawing an amazing amount of attention both by academics and industry due to their environment-friendly properties, and particularly their potential in green chemistry. The rapid growing number of publications and patents can be considered as the proof of the large amount of research and investment in this area and revealed their potential applicability and inspiring results [1,2]. ILs are salts, completely composed of ions with melting temperatures below 100 °C, a result of their low-charge density and low symmetry ions [1, 3-5]. ILs are categorised as ‘‘green’’ solvents thanks to their unique properties such as negligible vapour pressure, large range of temperatures at liquid stage[4], conventional non-flammability, non-volatility, and their outstanding solvation potential [2, 6-10]. Besides, due to their ionic character, most aprotic ILs display high thermal stability with decomposition temperatures around 300 - 500 °C, high chemical stabilities (extremely redox robustness), high ionic conductivity, and high solvation ability for organic, inorganic and organometallic compounds with improved selectivity [1-3, 11-14]. They are generally described as “designer solvents” and their potential is further extended due to the fact that their physical and chemical properties (such as their thermophysical properties, biodegradation ability or toxicological features, as well as their hydrophobicity and solution behaviours) may be delicately tuned by varying both the cation and the anion.[1, 3, 15-19].

Moreover, their tunable properties are enabling rapid advances in devices and processes for the production, storage and efficient use of energy. [1, 20]

However, for material applications, immobilising ILs in solid devices while keeping their specific properties is the main requirement being highly challenging [21]. Ionogels form a new class of hybrid materials which preserve the main properties of the ILs (liquid-like dynamics and ion mobility) but in a solid or gel like structure, while allowing easy shaping and thus, increasing considerably the potential use of ILs in key areas such as energy, environment and analysis. [21, 22] In the case of ionogels, a further dimension is achieved: the ability of keeping the ILs, and their properties, in a solid support, which can be called as "flexibility space" [21]. Moreover, the properties of the final ionogel are different from the simple combination of each pure component. Ionogels offer a way to further use ionic liquids in technological applications [22]. The combination of gels, with diversified applications of ionic liquids, enables the design of a thrilling combination of functional tailored materials, allowing materials to be custom designed for a wide range of applications such as sustainable chemistry, energy, electronics, medicine, food, cosmetics, among others [22].

"Lab-on-a-Chip" (LOC) or "micro-Total Analysis Systems" (μTAS) have the greatest potential of integrating multiple functional elements into a small device to produce truly sample-in/answer-out systems [23]. The design, fabrication, flow control, analysis and connection techniques are under continuous development improving among others, the throughput and the automation while at the same time leading to reduced costs [24]. However, the development of fully integrated microfluidic devices is still facing some significant obstacles, including the lack of robust fundamental building blocks for fluid control, the miniaturisation or elimination of external fluidic control elements [23, 25]. The control and movement of flows in microchannels

comes from microvalves and micropumps. In the case of active valves and pumps, the actuation depends on external power supplies and they require relatively complex procedures for integration into the microfluidic devices which mean a drawback for the device. On the other hand, passive valves/pumps have recently received huge amount of interest since they do not need any external actuation components and are easy to fabricate[24]. They can be seen as a response to the need of simple and effective fluid control elements for building low cost and sophisticated lab-on-a-chip devices. These valves are essentially fabricated from stimuli responsive polymer gels[24].Gels consisting of either physical or chemical cross-links can undergo controlled and reversible shape changes in response to an applied field [26]. In other words, they demonstrate substantial and reversible changes in equilibrium degree of swelling in response to weak changes in their surroundings (solvent composition, temperature, pH, and supply of electric field, light, etc.) [27-30]. They are referred as smart materials since they are able to perform functions by an external stimulus without the need of any human input, demonstrating potential for ‘‘smart” applications including biomedical devices, drug delivery carriers, scaffolds for tissue engineering, filters and membranes for selective diffusion, sensors for on-line process monitoring and artificial muscles among others [28, 31].

In particular ionogels can also be used as stimuli responsive gels. They have many advantages over conventional materials since their robustness, acid/ base character, viscosity and other critical operational characteristics can be finely modified through the tailoring of chemical and physical properties of the ILs[24]. The characteristics of the ionogels can be tuned by simply changing the IL and so the actuation behaviour when used as microvalves in microfluidic devices can be more precisely controlled [24, 32]. For instance, two interesting approaches developed by us

to control fluid movement in microfluidic devices are the use of photo-responsive ionogels controlled by light [33] and reversible thermoresponsive ionogel [34].

Although there have been significant developments and even promises in the microfluidics field yet, the amount of commercial products based on microfluidics is, with few exceptions, remained low due to the critical need of a large variety of costly high performance components (mixers, actuators, reactors, separators, valves and pumps etc.) for fluid control and transport in the devices. The increase of the cost of the devices resulted in the decrease of the market possibilities [35]. Therefore, "Lab on a paper" is being developed to provide an answer to deliver simple, cheap and autonomous devices which are easily manageable by the end-users [36]. These devices have the full potential of classical microfluidics but with a well-focused commercialisation path [37]. Paper is receiving a huge amount of attraction as a promising substrate material for microfluidic devices not only due to its extremely low cost and ubiquity but also due to its mechanical properties comprising flexibility, lightness, and low thickness[36]. In particular, µPADs is a relatively new group of analytical tools, capable of analysing complex biochemical samples, within one analytical run, where fluidic manipulations like transportation, sorting, mixing or separation are available[35, 38].

Thanks to the capillary forces of paper, there is no requirement for external pumps to provide fluid transport inside the paper unlike traditional microfluidic platforms[35]. However this advantage also generates a drawback; isotropic wicking behaviour of paper and the fluid transportation by any exposed surface area prevents the accurate control of the fluid transport on paper material, making it highly challenging and complicated [39, 40]. Lack of fluid control on paper is at this moment the main dragging force for researchers when looking for new capabilities of µPADs.

In our previous work [35], we had offered a solution by presenting a new concept for fluid flow manipulation in µPADs by introducing two different ionogel materials as passive pumps which were drop-casted at the inlets where the analytes are introduced into the device. It was demonstrated that ionogels highly affected the fluid flow by delaying the flow from the inlet. They revealed two distinctive liquid flow profiles due to their different physical and chemical properties and thus water holding capacities.

In this study, we extend our investigations and introduced another new concept for fluid flow manipulation in µPADs. Here, we use the ionogel materials as negative passive pumps at the outlet of the µPADs. The ionogel is able to continuously drive fluids through the µPAD by the swelling effect, and so to control the flow direction and flow volume that reach the outlet. In order to generate a useful, reproducible and operative device we investigated a new method for the integration of the ionogel materials into the µPADs. Finally, the characterisation and the performance of the ionogel as negative passive pump were carried out.

2. Experimental

2.1. Reagents and Materials

Whatman Filter paper Grade 1, wax printer XEROX ColourQube 8580 and a hot plate (Labnet International Inc., USA) were provided in order to fabricate the µPADs. The design of the devices was carried out with the software application AutoCAD™.

For the synthesis of the ionogels, *N*-isopropylacrylamide, *N*,*N*'-methylene-bis(acrylamide), 2,2-Dimethoxy-2-phenylacetophenone photoinitiator and 1-ethyl-3-methylimidazolium ethyl sulfate were purchased from Sigma-Aldrich, Spain. For gasket fabrication, cyclic olefin

copolymer (COP) was provided by Zeonex/Zeonor, Germany and the pressure sensitive adhesive layer (PSA) was gently provided by Adhesive Research, Ireland.

NaOH solution, and phenolphthalein, which are used for the observation of the colour change (pH) on the µPAD were provided by Sigma-Aldrich, Spain. For visual observation, blue food dye (McCormick, Sabadell, Spain) was used: 5 mL of water with 100 µL of food dye (high concentration).

2.2. Fabrication of the µPADs

The µPADs were fabricated using the wax printing method with standard laboratory filter paper. Firstly, the desired shape of the microfluidic was drawn in AutoCAD and then printed in one side of the paper. The final dimension of the microfluidic structure, borders and flow channels, are defined only when the wax is absorbed through the full thickness of the filter paper using the hot plate at the desired temperature. The best performance of the devices was obtained by heating the wax printed papers at 125 °C for 6 min.

2.3. Synthesis and integration of the ionogel

The ionogel used for fluid manipulation was obtained by mixing and heating *N*-isopropylacrylamide, *N*,*N*'-methylene-bis(acrylamide) and a photoinitiator (2,2-Dimethoxy-2-phenylacetophenone) dissolved in 1 mL of 1-ethyl-3-methylimidazolium ethyl sulfate ionic liquid, at 80 °C for 30 min following the same protocol describe before by us [35].The chemical structure of the ionogel and its position in the µPADs are illustrated in Figure 1.

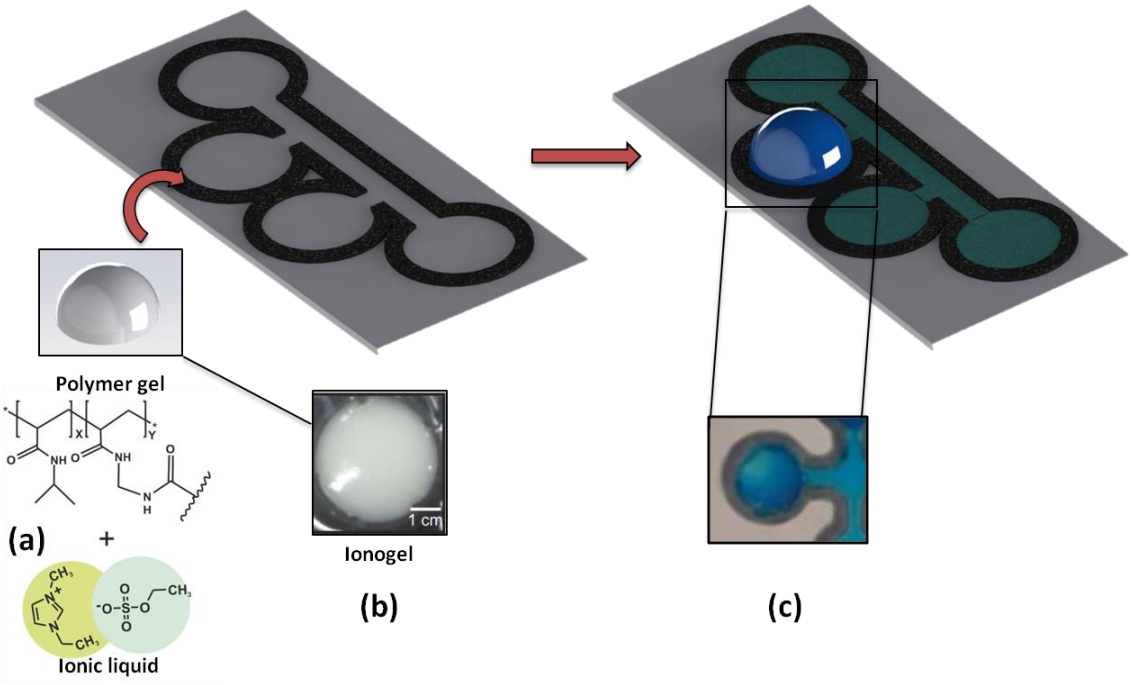

Figure 1. Scheme of the µPAD before and after ionogel integration. (A) Chemical structures of the components of the ionogel: polymer gel and 1-ethyl-3-methylimidazolium ionic liquid. (B): picture of the photopolymerised ionogel. (C) Picture of the hydrated ionogel using a blue dye water solution.

In order to define the shape of the ionogel on the paper device, a COP / PSA gasket was fabricated and adhered to the paper establishing the border of the gel during UV photopolymerisation. The gaskets have a square shape with dimensions of 20 x 20 mm and with a circle inside having a radius of 6 mm.

During the characterisation experiments 30 µL, 60 µL and 90 µL of the ionogel solution were drop-casted and instantly photopolymerised for 6, 12 and 16 min respectively, under 1600 mW cm^{-2} in three different circular outlets of the µPAD using the polymer gaskets. During the proof of concept experiments, 50 µL of the ionogel solution was drop-casted in the outlet of the

µPAD, using the gasket, and rapidly UV-photopolymerised for 10 min at 1600 mW cm^{-2}, see Figure 2.

In order to remove any unpolymerised material and excess of ionic liquid, the µPADs with ionogel were washed with deionised water (DI) for 2 min 7 times and let to dry at room temperature for 24 h.

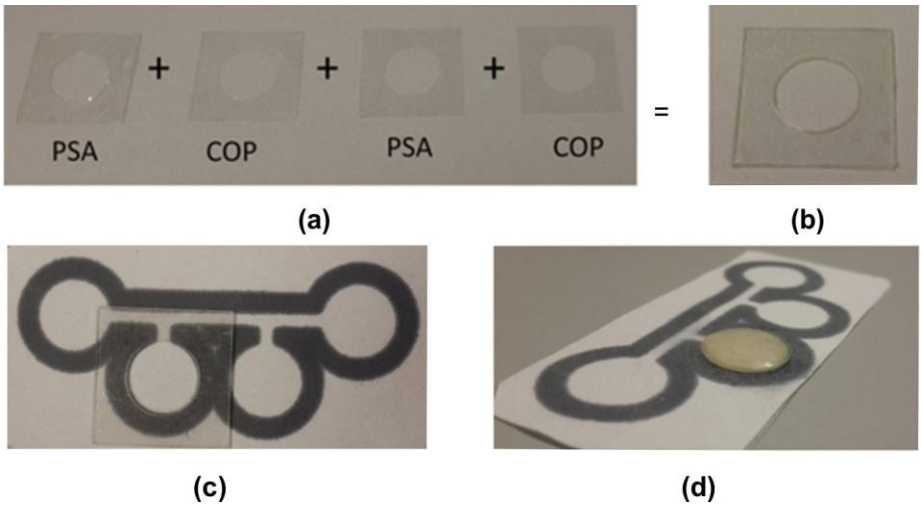

Figure 2. (a) COP and PSA layers and position to fabricate de gasket, **(b)** picture of the finalised gasket; **(c)** µPAD with adhered polymer gasket ready for the addition of the ionogel solution and subsequent UV photopolymerisation of the ionogel; **(d)** µPAD with a defined shaped ionogel after photopolymerisation and removal of the gasket.

2.4. Measurement protocols

During the characterisation experiments, 50 µL of blue dye (maximum volume that the inlet can hold without getting overloaded) was dropped in the middle inlet of a µPAD containing three outlets with 30 µL, 60 µL, 90 µL of photopolymerised ionogel solution and an outlet with no ionogel. This protocol was repeated 10 times to reach a total volume of 500 µL of blue dye solution in the µPAD. The fluid flow was recorded by a Samsung Galaxy Note3 camera. Photos

of the fluid behaviour of the µPAD, at different times, were extracted from a video and the volumes of the fluid absorbed by each ionogel were measured with a sensitive digital weight balance (Sartorius, Germany), after being removed from the µPAD using a cutter (these values include the weight of the paper below the ionogel).

During the proof of concept experiments, two type of straight channel µPADs having two perpendicular channels, two inlets and two outlets were used; one with no ionogel and another with the photopolymerised ionogel in one of the outlets. An equal volume (180 µL) of 1.2×10^{-2} M NaOH solution (pH = 12) and 1.2×10^{-2} M phenolphthalein solution (which has a fuchsia colour between pH = 10 and 13) were dropped onto the left and right inlets on both types of µPAD, respectively, simultaneously. The fluid flow behaviour was recorded by a Samsung Galaxy Note3 camera and the photos of their performance at different times were extracted from the video.

2.5. Interferometry and AFM measurement protocol

Interferometric images were taken with a Bruker contour GT optical microscope. The microscope has a fully automatic turret with an X, Y and Z movable stages. The droplets were imaged with a 5 X objective with a 0.55 X zoom lens. The ionogel was imaged at different times during 60 min. A JPK NanoWizard atomic force microscope in intermittent contact mode using a silicon tip ($r < 10$ nm; aspect ratio < 6 : 1) with a force constant of 40 N $m^{-1}$and a resonant frequency of approximately 300 kHz was employed to study the topography of the tested material.

In order to study the topography of the ionogel in the drying and swollen states, 20 µL of the ionogel were photopolymerised, washed with water and dried under vacuum overnight onto a

silicon wafer before measurements. The ionogel was rehydrated with 10 µL of water to study its swollen state.

2.6. Electrochemistry measurement protocol

Regarding the Cyclic voltammetry (CV) measurements, an electrochemical cell consisting of two Au interdigitated electrodes (deposited onto oxidised silicon substrate by RF magnetron sputtering according to literature) was used [41]. The cyclic voltammetry experiments were monitored with the Autolab electrochemical working station PGSTAT 302N using the Nova 1.9 software version (Eco Chemie). All cyclic voltammetry assays were performed under the same conditions using MilliQ water at room temperature. The measurements were carried out in a range between -3 V and 3 V, with a scan rate of 0.1 V/s.

3. Results

3.1. Fabrication of the µPADs

The wax printing method for µPAD fabrication is based on patterning hydrophobic barriers of wax in hydrophilic paper using a commercially available printer and a hot plate [42]. The fabrication process consisted of two core operations: (i) printing wax patterns on the paper surface with the wax printer and (ii) the penetration of the wax through the paper thickness by wax melting to form a complete hydrophobic barrier which defines the µPAD [42]. The µPAD fabrication followed the same protocol. Nevertheless, since the wax spreads through the paper during the heating process, it is necessary to investigate the relation between the heating temperature/ heating time and the final dimensions of the µPAD (width of the channel and width of the wax barriers) in order to have a homogeneous channel dimension for all the fabricated µPADs. It is obvious that the dimensions of the printed patterns on the paper do not directly

translate into the dimensions of the final hydrophobic patterns in the µPADs. The best performance was obtained with temperatures of 125 °C , higher temperatures damaged the shape of the printed patterns (wax is too liquefy and flows out of the defined patterns) while lower temperatures generated inhomogeneous transfer of the patterns and different widths dimensions on the wax barriers.

We founded out that the ideal heating time is that in which the wax barriers width of the top and back sides of the µPAD are equal so that the width of the final microfluidic channel is well defined and equal in width for all the fabricated devices. Figure 3 shows a set of experiments carried out at 125 °C varying exposition time. It can be observed that after 6 min both, the top and back channel widths are the same. Therefore, this fabrication protocol (temperature and time) was used for all the µPADs from now on. This homogeneous channel width ensures that the flow profile over the entire µPAD is the same. The channel width of the µPADs were measured (with a ruler) to be 0.30 mm ± 0.05 mm (n = 3).

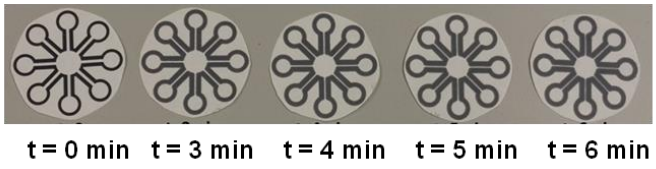

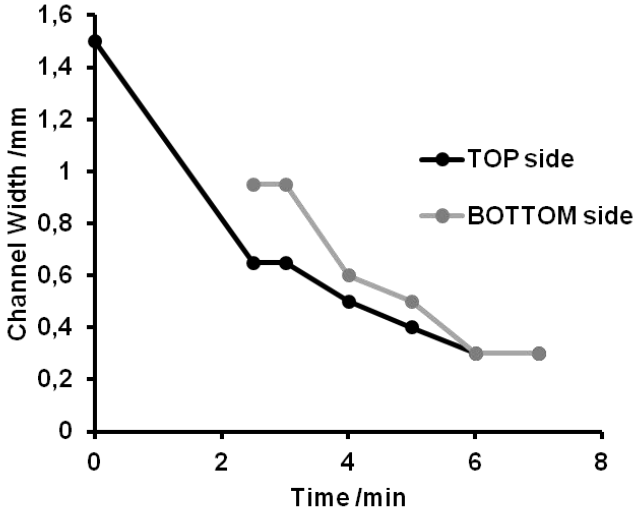

Figure 3. Pictures of a device at different heating times and graphical representation of the channel width at different heating steps during µPAD fabrication at 125 °C for 8 min (top and bottom sides of the µPAD). The bottom side is the one in contact with the heater.

3.3. Integration of the ionogel into the µPAD

In our previous publication[35] the integration of the ionogel, drop-casting and subsequent photopolymerisation, was carried out using the wax barriers as reservoirs to contend the ionogel solution during the photopolymerisation process. This protocol although effective, was not reproducible from device to device since it was a manual process. Moreover, it limited the volume of the ionogel that could be immobilised, since it was necessary to prevent the gel from spreading out of the wax barriers and through the channels. Another drawback was that the ionogel did not have a homogeneous shape for all the devices.

In this study, we developed a new technique, using a COP/PSA gasket, to accommodate the ionogel solution on top of the µPAD, to generate a homogeneous ionogel shape for all the devices after photopolymerisation and to extend the volume of the ionogel when integrated into the device.

The gasket was pasted to the paper through one of the PSA layers; this ensures that the gasket can be removed after photopolymerisation without peeling off the ionogel. The ionogel solution was photopolymerised, as soon as it was drop-casted onto the gasket. Using rapid photopolymerisation protocols, the spreading of the ionogel solution through the whole paper thickness was minimised [35] and the “sponge” structure of the ionogel, with the defined shape and borders, was generated on top of the paper, see Figure 2d.

After photopolymerisation and gasket removal, a short post heating step, 100 °C for 2 min, was necessary to regenerate the wax barriers. It was observed that during the drop-casting of the ionogel solution a small amount of wax can be dissolved into the ionogel solution and so generate small, microscopic, paths in the wax barriers for the liquid to break away from the µPAD. This heating step recovered the tightness of the barriers and did not vary the width channel dimensions (< 5 %). Finally a washing step was needed to remove all the unpolymerised material and excess of ionic liquid, see experimental section [34, 35].

3.4. Fluidic characterisation of the µPAD

In our previous publication, we demonstrated that the photopolymerised ionogels remained mainly on the surface of the paper and get physically attached mainly at the superficial paper fibers [35]. Therefore during the flow profile experiments it is expected that the liquid naturally flows through the paper fibers of the µPAD by the wicking properties of the hydrophilic paper and then, when liquid reaches the photopolymerised ionogel at the outlet, through the fibers, the negative pumping process of hydration of the ionogel starts taking place.

The ionogel solution volume was varied from 30 to 90 µL in the µPAD, and their fabrication performance and fluidic capabilities where investigated. The 30 µL and 60 µL ionogel µPADs were fabricated successfully and the ionogel did not peel off from the paper. However, the 40 % of the 90 µL ionogel µPADs investigated (n = 10), peeled off after photopolymerisation, thus those devices were useless. At volumes higher than 90 µL, the ionogel did not successfully attach to the paper surface because of the high excess of ionogel solution, therefore 90 µL was determined as the higher volume capable of generate an operative µPAD for our gasket and channel dimensions.

The fluid behaviour of a µPAD having different volumes of photopolymerised ionogel in three of its four outlets was investigated. The fluidic behaviour of the three ionogel negative pumps was observed and compared to each other. First, a 50 µL of coloured (blue) dye solution was injected into the inlet of the device, see Figure 4 a. The liquid coming from the inlet (centre of the µPAD) wets the paper and by the wicking mechanism of the paper it moved through the microfluidic channel to reach the outlets. Then, at the outlets the ionogel absorbe the liquid (hydration process) acting as a negative pump continously driving the liquid towards the outlets and leaving the inlet dry (Figure 4b). This process was repeated, five times, till the inlet reminded wet, ensuring that the three pumps were completely hydrated and so the flow stopped.

Visually it was possible to determine the times when the different negative pumps stop absorving liquid and so their actuation time was determined. At the outlet with no ionogel the wicking process finalised after 68 ± 2 min (n = 3) (Figure 4c). Then the outlet with 30 µL ionogel stoped acting as negative pump after 112 ± 4 min (n = 3) (Figure 4d) followed by the 60 µL ionogel outlet, 141 ± 4 min (n = 3) (Figure 4e), and finally the outlet with 90 µL ionogel, 146 ± 5 min (n = 3) (Figure 4f). Therefore the actuation time of the negative pumps can be regulated by varying the volume of the ionogel present at the outlet of the µPAD. The higher the volume is the longer the negative pump actuates.

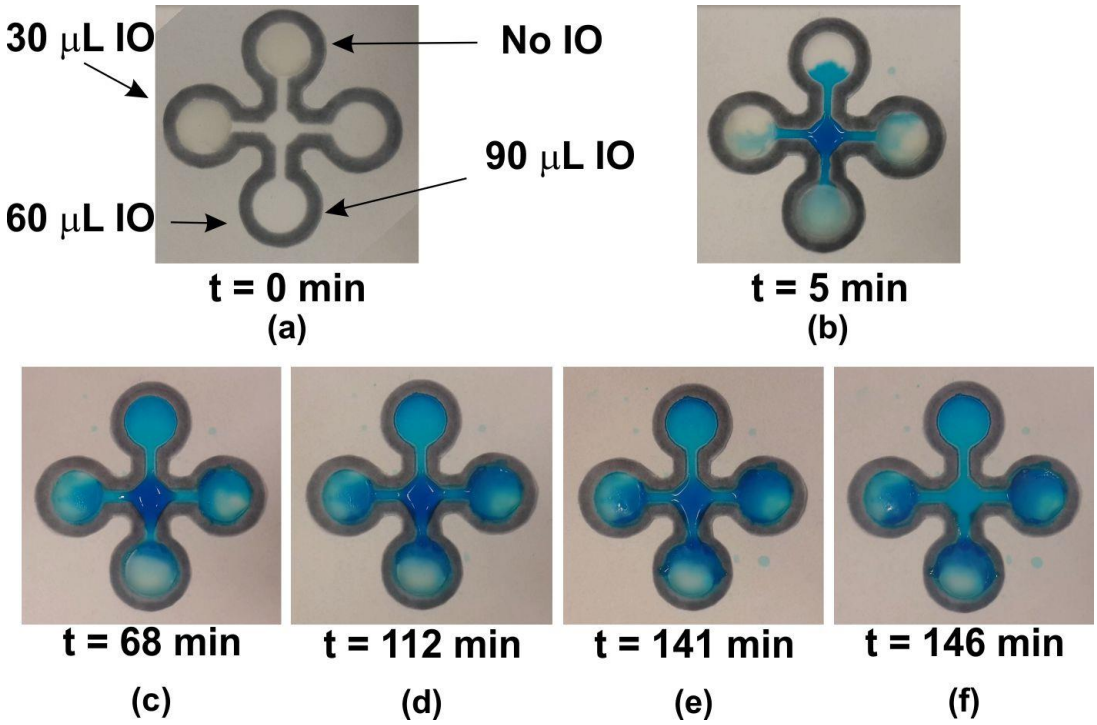

Figure 4. Actuation time of three different ionogel negative pumps in a single μPAD (ionogel volumes: 0, 30, 60 and 90 μL).

Figure 5 shows the swelling capability of each of the ionogels negative pumps. The volume of the photopolymerised ionogel in the outlet, highly affects the swelling degree of the ionogel and so the capability of the pump to absorb liquid into the μPAD. For instance, the 90 μL ionogel negative pump was able to absorb 107 ± 12 μL (n = 3) of blue dye solution while the bare paper is just able to absorb 17 ± 4 μL (n =3) for the same active area. This opens the possibility of modulating the actuation time of the negative pumps by just varying the volume of the photopolymerised ionogel, moreover these behaviour was found to be linear and consistent, small error, from device to device. It can be concluded that the wicking property of paper can be highly empowered by the addition of ionogel negative pumps, since gel material has a much higher capacity to absorb water than the bare paper material.

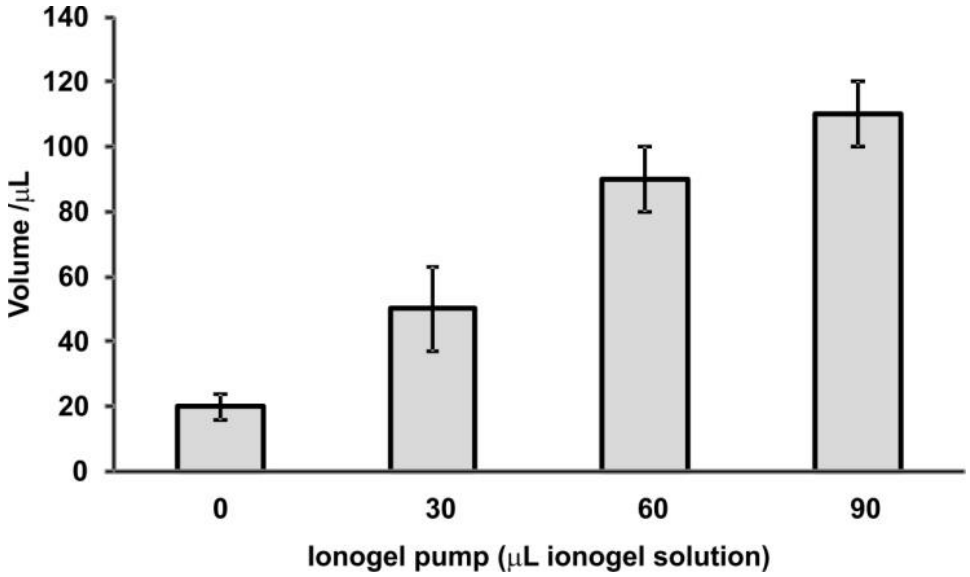

Figure 5. Water intake capability of the different negative ionogel negative pumps (n = 3).

Figure 6 shows a set of 3D images taken using a Bruker Contour microscope. The images show the morphology and the shape of the ionogel during the hydration process and its evolution over time. The surface of the ionogel is very porous at the dehydrated stage, with a topography presenting numerous cavities that can be observed in the AFM figures. The surface roughness calculated with the AFM images is 29 ± 6 nm. The pores can be found with different dimensions, providing the optimal conditions for water diffusion through the ionogel. When the hydration process starts, the topography of the ionogel varies significantly, the globular shapes of the surface increase in diameter as the ionogel swells. The increase in volume of the ionogel can be observed by comparing the first and the last pictures in Figure 6. The dimensions of pores are reduced and the surface of the ionogel presents higher irregularities with a roughness of 57 ± 7 nm (see AFM picture at the hydrated stage), growing in volume mainly in the *z*-axis direction. This could be attributed to the photopolymerisation process, where the restrictions made by the mold leave the ionogel just one degree of freedom in the *z*-axis direction, which becomes

predominant during hydration, as observed by us before [43]. These microscopic observations are in agreement with the behaviour observed by the ionogel negative pump in the µPAD.

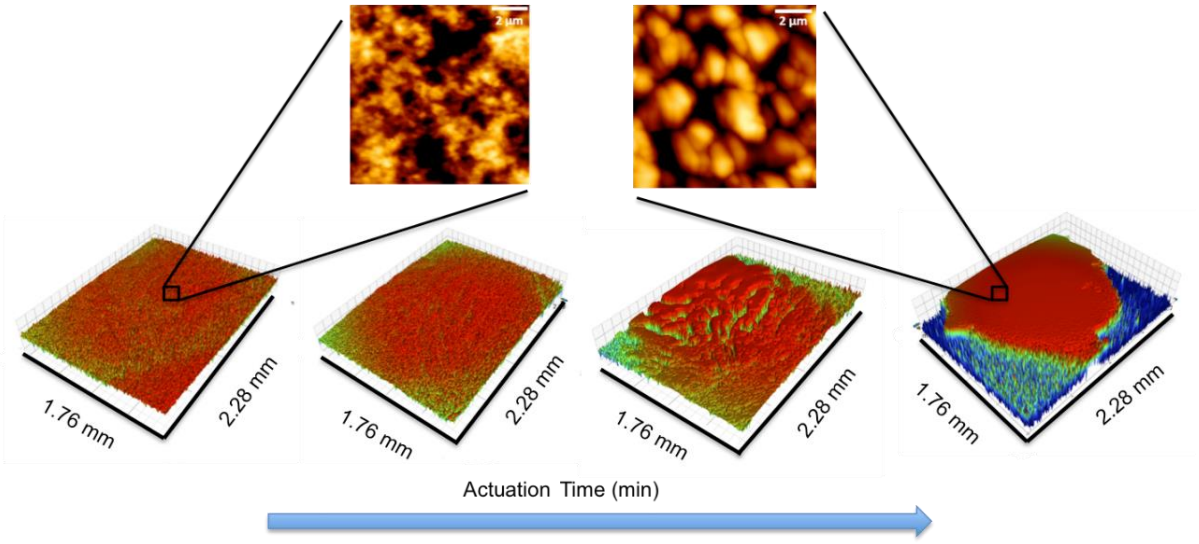

Figure 6. Top: AFM images of the dehydrated ionogel (left) and hydrated ionogel (right). Bottom: interferometric images at different times during the swelling process of the ionogel.

Cyclic Voltammetry is a commonly used technique to obtain information about the interactions between the ionogel and water molecules during the hydration process. Figure 7a shows a well-defined oxidation and reduction peak of the imidazolium cation with little or no presence of atmospheric moisture. The peaks appear at 1.194 and -1.189 V (ΔE = 2.38 V) and are related with the oxidation and the reduction of the cation of the ionic liquid. The ratio of the peak is almost one, which is indicative of the reversibility of the process [44]. Water was added to the ionogel for hydration, following the same protocol than above (figure7b). It can be observed that the process responsible for the narrowing of the electrochemical window that is associated with electrolysis of absorbed water in the hydration process does not occur when a two Au electrode system is used [45,46]. Therefore in both cases the voltammograms were typically scanned from +3 to -3 V. Moreover, there is a considerable shift of both cathodic and anodic peaks,

appearing at -0.46 V and 0.34, respectively (ΔE = -0.8 V). This can be explained considering that the swollen configuration of the hydrated ionogel favors the redox process of the imidazolium ions within the ionogel.

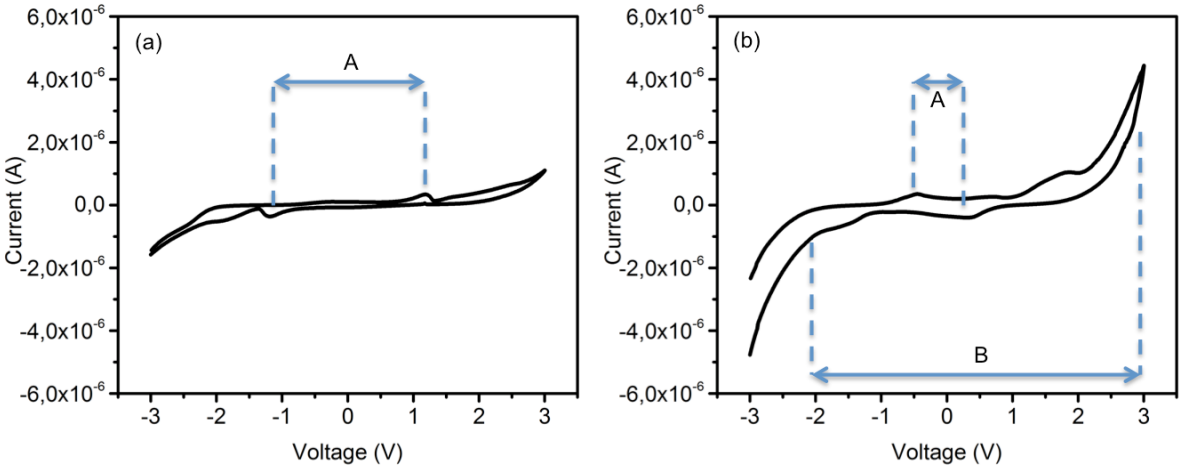

Figure 7. CV of the ionogel before (a) and after (b) the addition of water. The peaks marked with the A correspond to the redox peaks of the IO after and before the addition of water. The peaks marked with the B correspond to the water hydrolysis peaks.

3.5. Performance of the ionogel negative pumps.

As a proof of concept, the fluid flow manipulation capability of the ionogel negative pumps was investigated by comparing the mixing behaviour of two fluids on a µPAD with no ionogel pumps and a µPAD with an ionogel pump situated on one outlet. Two different solutions were injected into the µPAD inlets, simultaneously. On the right side inlet, a solution of NaOH (colourless, pH = 12) was injected, while on the left side inlet, a solution containing phenolphthalein pH indicator (yellow, giving fuchsia colour between pH = 10 and 13) was used. Both solutions flowed towards the centre of the µPAD thanks to the wicking properties of the paper.

In the case of the µPAD with no ionogel (Figure 8a), the mixing point was observed at the middle of the main channel (Figure 8a, picture 3) at t = 2.5 min. Then the wicking property of the paper ensures that both solutions flow towards their respective outlets at the same speed until the entire µPAD gets wet (Figure 8a, picture 4), t = 10 min. At that point, the wicking forces of the paper ended and therefore there were not any additional forces capable of moving the fluid towards any preferred direction. The mixing point was visualised through the formation of a fuchsia colour line at the interface of both solutions due to an abrupt change of pH expressed by the pH indicator (Figure 8a, picture 5 and 6) at t = 30 min. Then, the pink colour line spreads equally in both directions of the µPAD main channel, by diffusion (Figure 8a, picture 8).

In the case of the µPAD with the ionogel pump (Figure 8b) a different fluid behaviour was observed. First, the mixing point was observed on the left side of the main fluidic channel and not in the middle as occurred with the bare µPAD, at a t = 2 min (Figure 8b, picture 3). The location is slightly different than the one with no ionogel since the ionogel disturbs the expected flow behaviour. The hydration process of the ionogel is slower in time than the wicking process of paper; therefore the liquid on the right side of the µPAD flows faster in the main channel and meets the liquid coming from the left side (no ionogel pump) closer to it. The liquid on the left side needs to fill the reservoir with no ionogel so the liquid in the main channel gets delayed. Moreover, the visualisation of the mixing through the formation of the fuchsia line is not so well define since it happen at the interface of one of the outlets on the left side of the µPAD (Figure 8b, picture 4). Then, when the ionogel starts to hydrate, the negative pump commences to work. It is possible to observe that the mixing point of both fluids (fuchsia colour, red circle represented in Figure 8b) was driven towards the middle of the channel first, (Figure 8b, picture 5) and then to the right side of the µPAD, where the ionogel is located (Figure 8b, picture 6).

When the ionogel is hydrated, it can act as a positive pump releasing water from its matrix and wetting the main channel, since the channel is getting dry over time (55 min experiment at ambient conditions), pushing away the coloured plug from the ionogel region and so reaching the inlet, Figure 8b, picture 7. This behaviour would be something impossible to achieve with a conventional paper device. This mechanism can be explained following the hydration behaviour of the ionogel (swelling process, Figure 6) and considering that the water in-take and release of the ionogel depends on several parameters (1) physical interaction between paper and the gel, (in our case gel remained mainly on the paper surface and gets absorbed in the superficial paper-fibers, allowing the liquid to flow from the paper up to the gel), (2) the type of ionic liquid which highly determines the swelling behaviour of the ionogel (hydrophobicity or hydrophilicity), (3) the porosity level of the gel structure (important for accommodation and release of water), and (4) the geometry of the gel [35].

Therefore, the flow behaviour on a μPAD was modulated on desired by introducing the swelling capabilities of the ionogel which acts as negative passive pump. It was proven that it is possible to control the flow direction and even reverse the flow, on a μPAD by applying the ionogel negative passive pump in a simple manner.

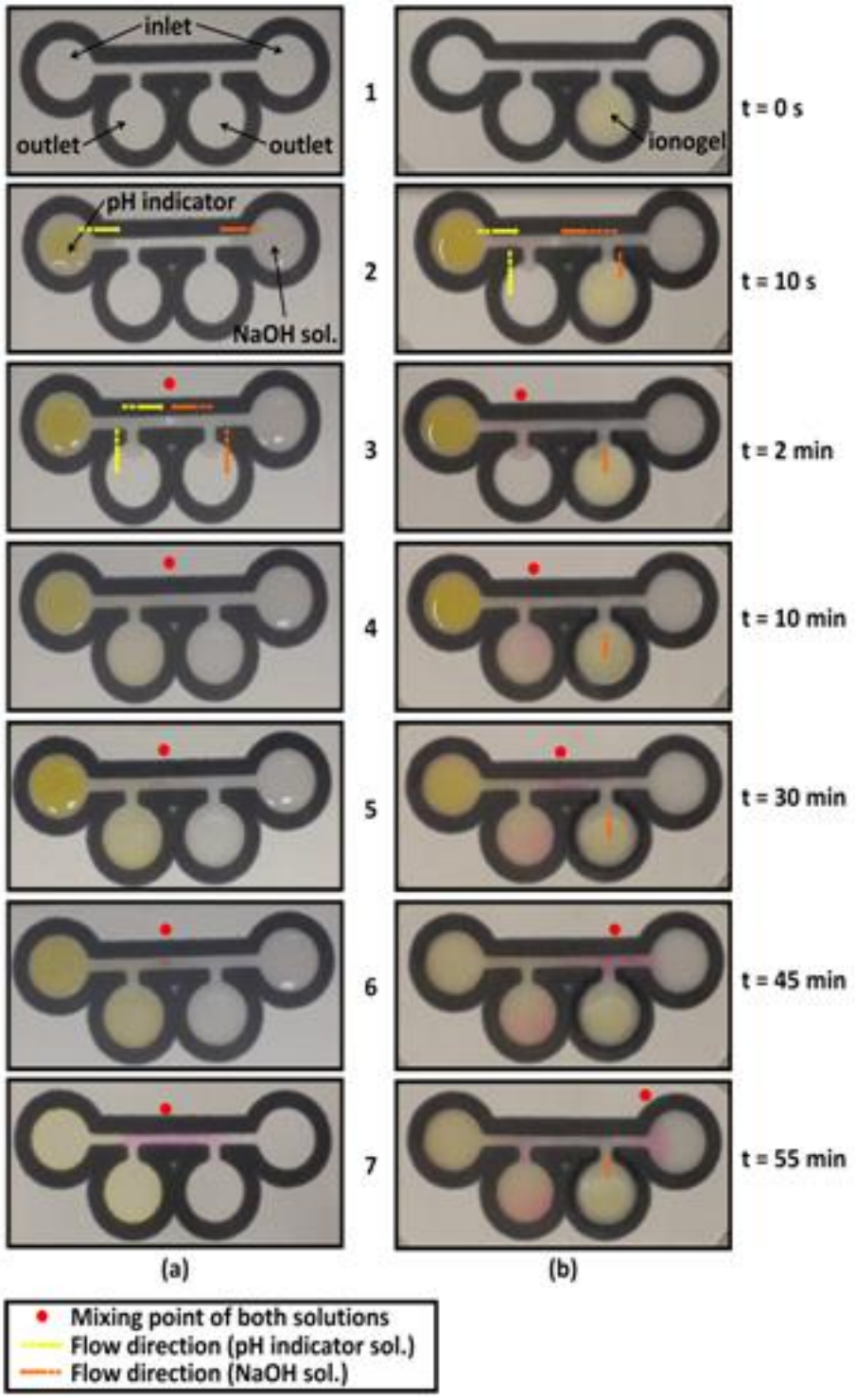

Figure 8. (a) Pictures showing the fluidic behaviour of a conventional µPAD over time (wicking forces). **(b)** Pictures showing the fluidic behaviour of a µPAD with an ionogel negative passive pump.

4. Conclusions

In this contribution a 1-ethyl-3-methylimidazolium ethyl sulfate ionogel was used as a material for the fabrication of negative passive pumps in µPADs. The integration of a COP/PSA gasket during the fabrication protocol allowed for shaping the ionogel and therefore ensured the integration of different volumes of ionogel in a single µPADs. Moreover the gasket allowed for the fabrication of homogeneous ionogel shapes which minimised possible manual fabrication errors.

The flow behaviour of the µPADs can be modulated, redirected an even reverse in the presence of the ionogel negative passive pump. This flow control is possible when the wicking process on the paper has finalised and can be extended on time till the hydration of the ionogel has reached completion.

This behaviour is reproducible, the same flow profile was observed in all the µPAD fabricated (n = 6). The only difference observed among them was the mixing time (± 60 s, n = 6), which differs from device to device and can be explained due to the irregular widths obtained during the fabrication process (5% of error). Another difference was observed in the flow speed generated by the ionogel negative pump (observed by the displacement of the fuchsia mixing point through the main channel), ~ 20 % error. These can be attributed to the small differences in ionogel volume present in the µPAD, since the drop-casting, photopolymerisation and washing steps of the process are manually done.

This investigation guaranties the use of ionogel negative passive pumps in µPADs for many applications in a simple manner without the need of external pumps. It will open the

possibility to detect analytes, sequentially and independently from the main μPAD channel wicking forces, without the need to design complicated 3D configurations.

5. Acknowledgments

The project was carried out with the support of the Ramón y Cajal programme (Ministerio de Economía y Competitividad). FBL thanks to the European Union‘s Seventh Framework Programme (FP7) for Research, Technological Development and Demonstration under grant agreement no. 604241 and the Gobierno Vasco, Dpto. Industria, Innovación, Comercio y Turismo under ELKARTEK KK-2015/00088. FBL and TA personally acknowledge Marian M. de Pancorbo for letting them to use her laboratory facilities at UPV/EHU. MCMM acknowledges the Basque Government under the Etortek Program (Grant No. IE14–391). NG-G work was supported by a PhD fellowship from the University of Navarra. Authors also acknowledge Adhesive Research for the donation of the PSA samples.

5. References

[1] M. Petkovic, K. R. Seddon, L. P. N. Rebelo, C. S. Pereira, Ionic liquids: a pathway to environmental acceptability, Chem. Soc. Rev. 40 (2011) 1383-1403.

[2] S. Zhang, J. Wang, X. Lu, Q. Zhou (Eds.), Structures and Interactions of Ionic Liquids 115, in: D. M. P. Mingos (Series Ed.) Structures and Bonding, Springer-Verlag, Berlin-Heidelberg, 2014, pp.1-197.

[3] H. Passos, M. G. Freire, J. A. P. Coutinho, Ionic liquid solutions as extractive solvents for value-added compounds from biomass, Green Chem. 16 (2014) 4786-4815.

[4] A. Stark, K.R. Seddon, Ionic liquids, in: A. Seidel (Ed.), Kirk-Othmer Encyclopaedia of Chemical Technology 26, John Wiley & Sons, Inc., Hoboken, New Jersey, 2007, pp. 836-920.

[5] K. R. Seddon, Ionic Liquids for Clean Technology, J. Chem. Technol. Biotechnol. 68 (1997) 351-356.

[6] N. V. Plechkova, K. R. Seddon, Applications of ionic liquids in the chemical Industry, Chem. Soc. Rev. 37 (2008) 123-150.

[7] C. C. Weber, A. F. Masters, T. Maschmeyer, Structural features of ionic liquids: consequences for material preparation and organic reactivity, Green Chem. 15 (2013) 2655-2679.

[8] M. J. Earle, J. M. S. S. Esperanca, M. A. Gilea, J. N Canongia- Lopes, L. P. N. Rebelo, J. W. Magee, K. R. Seddon and J. A. Widegren, The distillation and volatility of ionic liquids, Nature 439 (2006) 831-834.

[9] J. Dupont, P. A. Suarez, A. P. Umpierre, Organo-zincate molten salts as immobilising agents for organometallic catalysis, Catal. Lett. 73 (2000) 211-213.

[10] J. S. Wilkes, A short history of ionic liquids—from molten salts to neoteric solvents, Green Chem. 4 (2002) 73-80.

[11] J. M. S. S. Esperanca, J. N. Canongia Lopes, M. Tariq, L. M. N. B. F. Santos, J. W. Magee, L. P. N. Rebelo, Volatility of aprotic ionic liquids—a review, J. Chem. Eng. Data 55 (2010) 3-12.

[12] R. D. Rogers, K. R. Seddon, Ionic liquids—solvents of the future? Science 302 (2003) 792-793.

[13] F. Guo, S. Zhang, J. Wang, B. Teng, T. Zhang, M. Fan, Synthesis and applications of ionic liquids in clean energy and environment: a review, Curr. Org. Chem. 19 (2015) 455-468.

[14] J. Zhang, A. Bond, Practical considerations associated with voltammetric studies in room temperature ionic liquids, Analyst 130 (2005) 1132-1147.

[15] L. P. N. Rebelo, J. N. C. Lopes, J. M. S. S. Esperanca, H. J. R. Guedes, J. Lachwa, V. Najdanovic-Visak and Z. P. Visak, Accounting for the unique, doubly dual nature of ionic liquids from a molecular thermodynamic and modeling standpoint, Acc. Chem. Res. 40 (2007) 1114-1121.

[16] T. Welton, Room temperature ionic liquids: solvents for synthesis and catalysis, Chem. Rev. 99 (1999) 2071-2083.

[17] R. D. Rogers, K. R. Seddon, Ionic liquids 11 IB: Fundamentals, Progress, Challenges, and Opportunities, American Chemical Society Symposium Series, Washington D.C, 2005.

[18] J. Ranke, S. Stolte, R. Stoermann, J. Arning, B. Jastorff, Design of sustainable chemical products—the example of ionic liquids, Chem. Rev. 107 (2007) 2183-2206.

[19] M. Earle, K. Seddon, Ionic liquids, green solvents for the future, Pure Appl. Chem. 72 (2000) 1391-1398.

[20] J. F. Wishart, Energy applications of ionic liquids, Energy Environ. Sci. 2 (2009) 956- 961.

[21] J. Le Bideau, L. Viau, A. Vioux, Ionogels, ionic liquid based hybrid materials, Chem. Soc. Rev. 40 (2011) 907-925.

[22] P. C. Marr, A. C. Marr, Ionic liquid gel materials: applications in green and sustainable chemistry Green Chem. 18 (2016) 105-128.

[23] C. T. Culbertson, T. G. Mickleburgh, S. A. Stewart-James, K. A. Sellens, M. Pressnall, Anal. Chem. 86 (2014) 95-118.

[24] M. Czugala, B. Ziolkowski, R. Byrne, D. Diamond, F. Benito-Lopez, Materials science: the key to revolutionary breakthroughs in micro-fluidic devices, Proceedings SPIE, Nano-Opto-Mechanical Systems, 8107 (2011) 81070C.

[25] R. Byrne, F. Benito-Lopez, D. Diamond, Materials science and the sensor revolution, Mater. Today 13 (2010) 16-23.

[26] S. Ahn, R. M. Kasi, S. Kim, N. Sharma, Y. Zhou, Stimuli-responsive polymer gels, Soft Matter 4 (2008) 1151-1157.

[27] R. R. Yoshida, T. Okano, Stimuli-responsive hydrogels and their application to functional materials, in: M. Ottenbrite, K. Park, T. Okano (Eds.), Biomedical Applications of Hydrogels Handbook, Springer, New York, 2010, pp. 19-43.

[28] A. D. Drozdov, C. -G. Sanporean, J. D. Christiansen, Modeling the effects of temperature and pH on swelling of stimuli-responsive gels, Eur. Polym. J. 73 (2015) 278-296.

[29] M. Irie, Stimuli-responsive Poly(N-isopropyl- acrylamide) photo- and chemicals-induced phases transitions, in: K. Dusek (Ed.), Responsive Gels: Volume Transitions: II, Springer-Verlag, Berlin and Heidelberg, 2013, pp. 63-85.

Masahiro Irie "Stimuli-Responsive Poly(N-isopropyl- acrylamide), Photo- and Chemicals-Induced Phases Transitions[30] E. M. White, J. Yatvin, J. B. Grubbs III, J. A. Bilbrey, J. Locklin, Advances in smart materials: stimuli-responsive hydrogel thin films, J. Polym. Sci. Part B: Polym. Phys. 51 (2013) 1084-1099.

[31] M. A. C. Stuart, W. T. S. Huck, J. Genzer, M. Mueller, C. Ober, M. Stamm, G. B. Sukhorukov, I. Szleifer, V. V. Tsukruk, M. Urban, F. Winnik, S. Zauscher, I. Luzinov and S. Minko, Emerging applications of stimuli-responsive polymer materials, Nat. Mater. 9 (2010) 101-113.

[32] A. Kavanagh, R. Byrne, D. Diamond, K. J. Fraser, Stimuli responsive ionogels for sensing applications-an overview, Membranes 2 (2012) 16-39.

[33] F. Benito-Lopez, R. Byrne, A. M. Raduta, N. E. Vrana, G. McGuinness, D. Diamond, Ionogel-based light-actuated valves for controlling liquid flow in micro-fluidic manifolds, Lab Chip 10 (2010) 195-201.

[34] F. Benito-Lopez, M. Antoñana-Diez, V. F. Curto, D. Diamond, V. Castro-Lopez, Modular microfluidic valve structures based on reversible thermoresponsive ionogel actuators, Lab Chip 14 (2014) 3530-3538.

[35] T. Akyazi, J. Saez, J. Elizalde, F. Benito-Lopez, Fluidic flow delay by ionogel passive pumps in microfluidic paper-based analytical devices, Sens. Actuators B 233 (2016) 402-408.

[36] E. Fu, T. Liang, P. Spicar-Mihalic, J. Houghtaling, S. Ramachandran, P. Yager, Two-dimensional paper network format that enables simple multistep assays for use in low-resource settings in the context of malaria antigen detection, Anal. Chem. 84 (2012) 4574-4579.

[37] E. Livak-Dahl, I. Sinn, M. Burns, Microfluidic chemical analysis systems, Annu. Rev. Chem. Biomol. Eng. 2 (2011) 325-353.

[38] P. Lisowski, P. K. Zarzycki, Microfluidic paper-based analytical devices (μPADs) and micro total analysis systems (μTAS): development, applications and future trends, Chromatographia 76 (2013) 1201-1214.

[39] C. R. Mace, R. N. Deraney, Manufacturing prototypes for paper-based diagnostic devices, Microfluid. Nanofluid. 16 (2014) 16, 801-809.

[40] A. Boehm, F. Carstens, C. Trieb, S. Schabel, M. Biesalski, Engineering microfluidic papers: effect of fiber source and paper sheet properties on capillary-driven fluid flow, Microfluid. Nanofluid. 16 (2014) 789-799.

[41] L. Rojo, I. Castro-Hurtado, M. C. Morant-Miñana, G. G. Mandayo, E.Castaño, Enhanced features of Li2CO3 sputtered thin films induced by thickness and annealing time, Cryst.Eng.Comm. 17 (2015) 1597-1602**.**

[42] E. Carrilho, A. W. Martinez, G. M. Whitesides, Understanding wax printing: a simple micropatterning process for paper-based microfluidics, Anal. Chem. 81 (2009) 7091-7095.

[43] M. Czugala, C. O'Connel, C. Blin, P. Fischer, K. J. Fraser, F. Benito-Lopez, D. Diamond, Swelling and shrinking behaviour of photoresponsive phosphonium-based ionogel microstructures, Sens. Actuators B 194 (2014) 105-113.

[44] A. Zuzuarregui, M. C. Morant-Miñana, E. Pérez-Lorenzo, G. Martínez de Tejada, S. Arana, and M. Mujika, IEEE Sens. J. 14 (2014) 270-277.

[45] U. Schröder, J. D. Wadhawan, R. G. Compton, F. Marken, P. A. Z. Suarez, C. S. Consorti, R. F. de Souza, J. Dupont, Water-induced accelerated ion diffusion: voltammetric studies in 1-methyl-3-[2,6-(S)-dimethylocten-2-yl]imidazolium tetrafluoroborate, 1-butyl-3-methylimidazolium tetrafluoroborate and hexafluorophosphate ionic liquids, New J. Chem. 24 (2000) 1009-1015.

[46] A. M. O'Mahony, D. S. Silvester, L. Aldous, C. Hardacre, R. G. Compton, Effect of water on the electrochemical window and potential limits of room-temperature ionic liquids J. Chem. Eng. Data 53 (2008) 2884–2891.